

Numerical Simulation of Ethylene Fueled Scramjet Combustor with Air Throttling, Part2: Transient Details*

Jeong-Yeol Choi^{a,*} · Jinhyeon Noh^{ab} · Seung-Min Jeong^a · Jae-Eun Kim^a · Vigor Yang^c

^aDepartment of Aerospace Engineering, Pusan National University, Busan 46241, Korea

^bPresently at Pangyo R&D Center, Hanwha Power Systems CO, Gyeonggi-do 13488, Korea

^cDaniel Guggenheim School of Aerospace Engineering, Georgia Institute of Technology, Atlanta, GA 30332, U.S.A.

Corresponding author *

Jeong-Yeol Choi
aerochoi@pusan.ac.kr

Received : 6 October 2020

Revised : 11 June 2021

Accepted : 18 June 2021

* Present paper is the revised version of AIAA 2011-2395 presented at 17th AIAA International Space Planes and Hypersonic Systems and Technologies Conference, 11 - 14 April 2011, San Francisco, CA, U.S.A.

A high-resolution numerical study is carried out to investigate the transient process of the fuel injection, combustion, and the shock-train formation by air-throttling in the isolator of an ethylene-fueled direct-connect scramjet combustor. The transient simulation begins with the supersonic air flow development followed by fuel injection. Air-throttling is then applied at the expansion part of the combustor to provide mass addition to block the flow to subsonic speed. The ignition occurs several milliseconds later when the fuel and air are mixed sufficiently. The pressure buildup by the combustion leads to the shock-train formation in the isolator section that advances to the exit of the facility nozzle. Then, the air-throttling is deactivated, the exhaust process begins and the situation before the air-throttling is restored. Present simulation shows the detailed processes in the dual mode scramjet combustor for better understanding of the operation regimes and characteristics.

Key Words: Supersonic Combustion, Dual Mode Scramjet, Air throttling, Shock Interaction, Ignition Transients

1. Introduction

Air-breathing hypersonic propulsion based on supersonic combustion has been studied for more than 50 years and has proved its potential through the hydrogen-fueled Hyshot and X-43A [1], hydrocarbon-fueled X-51A, and HyFly flight test programs [2]. Hydrocarbon fuels have higher volumetric energy density; thus its use makes the scramjet engine much more efficient. Hydrogen, on the other hand, has higher energy per unit mass, higher propulsion performance, higher heat cooling capacity, and higher flame speed, and superior ignition characteristics. Hydrogen engines are considered as viable propulsion options for space travel, whereas hydrocarbon engines are useful mainly for atmospheric flight.

Copyright © 2021 The Korean Society of Propulsion Engineers

© This is an Open-Access article distributed under the terms of the Creative Commons Attribution Non-Commercial License (<http://creativecommons.org/licenses/by-nc/3.0>) which permits unrestricted non-commercial use, distribution, and reproduction in any medium, provided the original work is properly cited.

One of the major obstacles in using a hydrocarbon fuel is its low flame speed, which renders it difficult to achieve complete combustion within the limited flow residence time (order of 1 ms) in a scramjet engine. The situation is further exacerbated for liquid fuels due to the time needed for atomization and evaporation. Thus, the liquid fuel is typically preheated to its supercritical state in the cooling passage. At the same time, it is cracked down to lighter species such as ethylene to have better cooling characteristics, since the process is endothermic and can absorb additional heat [3]. Although a variety of species in cracked kerosene fuel may exist, ethylene, C_2H_4 apparently is the dominant ingredient since its C/H ratio of 1/2 is very close to that of kerosene. Regardless of gasification of the fuel, the combustion of the hydrocarbon as scramjet fuel is still difficult due to its low flame speed.

To improve the ignition and combustion characteristics of hydrocarbon scramjet engines, several flow choking devices were employed at the end of the combustor [4]. Among them, the air throttling technique makes a temporary throat aerodynamically by injecting air at the end of the combustor [5]. Thus, the combustion enhancement by the air throttling is worth investigating by numerical means for further optimization of hydrocarbon scramjet engine system.

This research studies the transient process of flow establishment and combustion process for an ethylene-fueled direct-connect scramjet combustor operating at dual-mode (ramjet mode - subsonic combustion and scramjet mode - supersonic combustion) with air-throttling. This work is an extension of previous work [6,7] with finer resolution to investigate detailed flow structures during the transient process.

2. Simulation Model and Numerical Approaches

2.1 Physical Models and Numerical Approaches

The flowfield is assumed to be two-dimensional for computational efficiency offering very fine resolution over the entire system and long operation time to investigate overall characteristics. The coupled form of species conservation, fluid dynamics, and turbulent transport equations can be summarized in a conservative vector form as follows.

$$\frac{\partial \mathbf{Q}}{\partial t} + \frac{\partial \mathbf{E}}{\partial x} + \frac{\partial \mathbf{F}}{\partial y} = \frac{\partial \mathbf{E}_v}{\partial x} + \frac{\partial \mathbf{F}_v}{\partial y} + \mathbf{W} \quad (1)$$

where,

Here, total density ρ is expressed as a sum of the partial density ρ_j of each species, u and v are velocity components, and e is total energy per unit volume. Pressure p is evaluated from the ideal gas law for a mixture of thermally perfect gases. Last two equations are turbulence transports equations where k is turbulent kinetic energy and ω is turbulent vorticity. Further details of the governing equations are described in the previous works [7-10]. The vector \mathbf{Q} is a conservative variable vector and the vector \mathbf{W} is a source term vector. Convective flux vector \mathbf{E} and \mathbf{F} are discretized by the Roe's flux difference splitting (FDS) method and viscous flux vector \mathbf{F}_v and \mathbf{G}_v are discretized by central difference method. The computational code has been used before for a supersonic combustor study [7,8] and currently extends to fifth order accurate scheme.[9]

$$\mathbf{Q} = \begin{bmatrix} \rho_j \\ \rho u \\ \rho v \\ \rho e \\ \rho k \\ \rho \omega \end{bmatrix}, \mathbf{E} = \begin{bmatrix} \rho_j u \\ \rho u^2 + p \\ \rho uv \\ (e+p)u \\ \rho uk \\ \rho u \omega \end{bmatrix}, \mathbf{F} = \begin{bmatrix} \rho_j v \\ \rho uv \\ \rho v^2 + p \\ (e+p)v \\ \rho vk \\ \rho v \omega \end{bmatrix}, \mathbf{E}_v = \begin{bmatrix} -\rho_j u_j^d \\ \tau_{xx} \\ \tau_{xy} \\ \beta_x \\ \mu_k \partial k / \partial x \\ \mu_k \partial \omega / \partial x \end{bmatrix}, \mathbf{F}_v = \begin{bmatrix} -\rho_j v_j^d \\ \tau_{yx} \\ \tau_{yy} \\ \beta_y \\ \mu_k \partial k / \partial y \\ \mu_k \partial \omega / \partial y \end{bmatrix}, \mathbf{W} = \begin{bmatrix} \omega_j \\ 0 \\ 0 \\ 0 \\ S_k \\ S_\omega \end{bmatrix} \quad (2)$$

Three-dimensional simulation is much more realistic for the study turbulent combustion and flow physics [9,10], but two-dimensional assumption is employed in this study for the tolerable computation time for the simulation of long-time operation. Menter's shear stress transport (SST) model is used with SST DES (detached eddy simulation) extension [11] to enhance eddy capturing characteristics at separated flow region while preserving the RANS characteristics at boundary layer. The second order implicit time integration is used with sub-iterations for time accurate computation. The two-dimensional code is parallelized by OpenMP for the optimum performance in multi-core SMP (shared memory processors) machines.

The subscript j denotes reaction species, O, O₂, H, H₂, OH, H₂O, CO, CO₂, C₂H₄, N₂. Nitrogen is regarded as inert gas since it has little effects on chemical kinetics and heat of reaction. For the ethylene reaction mechanism, modified version of Singh and Jachimowski's quasi-global chemistry mechanism, which involves 10 elementary reaction steps and 8 reaction species [6]. It predicts the equilibrium condition with higher accuracy than does the global chemistry model by including intermediate species. Validity of the mechanism is addressed in the previous work [6,7], and the code used for present study has been validated through a number of previous works by authors group [6-10,12].

2.2 Direct-Connect Supersonic Combustor Configuration

Figure 1 shows the schematics of direct-connect supersonic flow test facility considered in this study [13]. It measures a length of 178.9 cm and consists of a facility nozzle, an isolator, a combustor, and an exhaust nozzle.

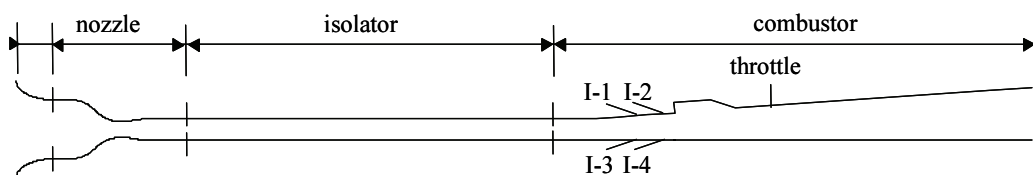


Fig. 1. Schematics of the direct-connect scramjet combustor [13].

The isolator is 3.81 cm high. Simulated flight Mach number covers the range of 3.5 to 6.0, and the dynamic pressure varies from 24 to 96 kPa. Fuel injectors are designated as I-1 through I-4 in Fig. 1, those are mounted on the top and bottom walls of the combustor at $x=106$ and 111 cm, respectively. In the present two-dimensional numerical simulations, circular injectors are replaced by slit injectors while maintaining the equivalent injection area. The specific geometry is determined by the fuel mass flow rate. The cavity flame holder starts from 116 cm. Its depth is 1.7 cm, and the upper and lower lengths are 5 and 10 cm, respectively. The combustor wall diverges 2.6 degree upward, while the bottom wall remains flat.

2.3 Computational Conditions

Numerical simulations is carried out under flight condition of Mach 5 and dynamic pressure of 24 kPa. The mass flow rate of the inlet air is 0.757 kg/s, the static temperature is 1,050 K and the static pressure is 3.744 atm. The Mach number, static temperature and static pressure at the exit of the facility nozzle are 2.22, 560 K and 0.328 atm, respectively. No-lip adiabatic condition is applied along the walls. Gaseous ethylene is injected into the combustor after the air flow is stabilized. The ethylene mass flow rate is 0.052 kg/s, corresponding to equivalence ratio of 1.0. Ethylene fuel is injected under Mach number 1.66, static temperature 520 K and static pressure 26.4 kPa. Air throttle is mounted at the top of the combustor wall at $x=136$ cm which injected 0.151 kg/s air vertically downward at 1 ms after the fuel injection. All flow conditions are summarized in Table 1.

The computation domain is covered by 2,415×151 grid

for main combustor and 300×121 grid for cavity region. The grid convergence study has been reported in the previous work [9], but twice finer resolution in flow direction and 1.5 times finer resolution in transverse direction are used to capture the finer details of flow structures.

Table 1. Operation condition of the scramjet combustor [7].

	Static Temperature	Static Pressure	Mach No.	Injection Angles
Nozzle inlet	1,050 K	382.4 kPa	0.097	
Isolator inlet	560 K	33.2 kPa	2.22	
Fuel injection	520 K	26.4 kPa	1.66	75°
Air throttle	273 K	194.5 kPa	1.00	90°

3. Results and Discussion

3.1 Transient process of the combustor operation

The transient simulation begins with the supersonic air flow development by applying the low-pressure condition at the right exit. Supersonic extrapolation boundary condition is applied after supersonic flow is established. The sequence of the flow establishment process is plotted in Fig. 2 and 3. Fuel injection time is set to 0.0 ms. Thus, the plots at $t=0.0$ ms show the stabilized non-reacting flow field just before the fuel injection. Due to the flow oscillation by the presence of the cavity, the flow is not at completely steady state. At 1.5 ms after the fuel injection,

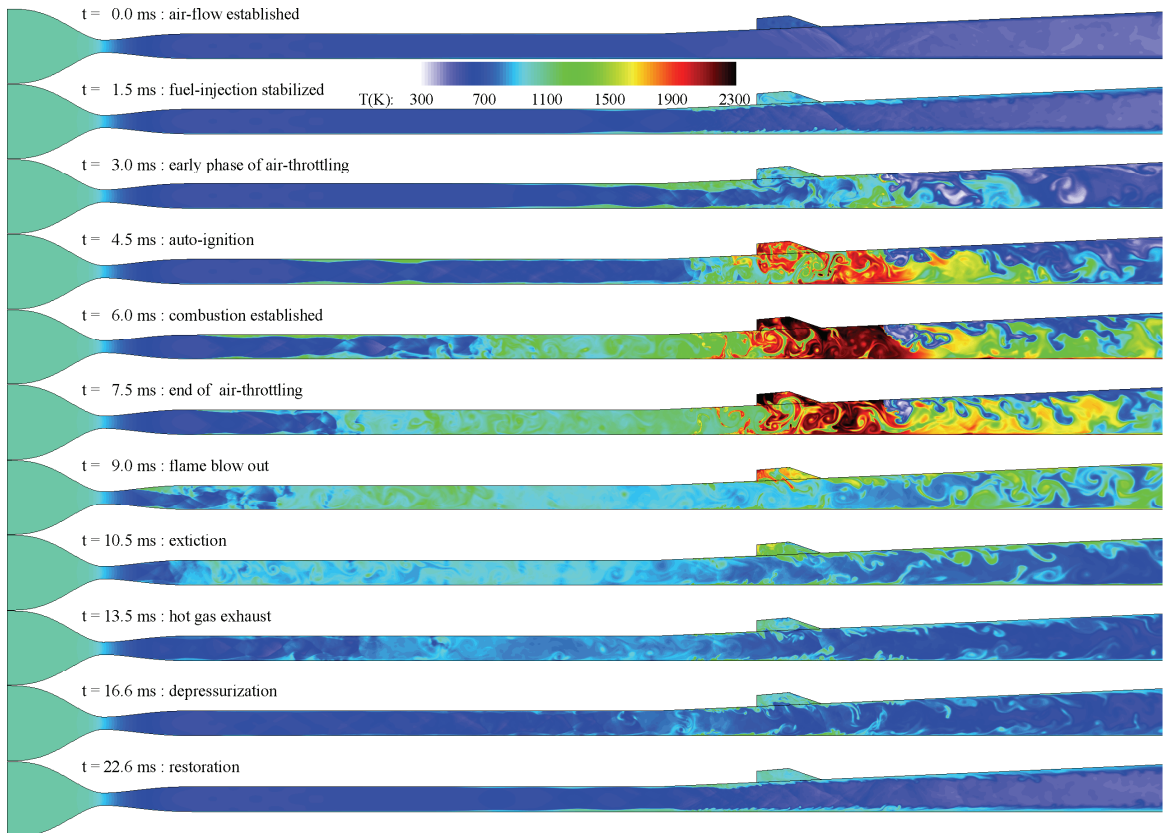


Fig. 2. Transients of temperature distributions.

fuel is layered along the combustor upper and lower surface walls. Different from the case of hydrogen injection studies in previous study [6], the fuel neither mixed with air, nor ignited, although there is a fluctuation at the surface of the fuel layer. It is consistent with the lower resolution case studies before.

Air-throttling is applied hereafter. 1.5 ms after the air-throttling (3.0 ms after the fuel injection) it is shown that the temperature and pressure rose within the combustor. It is considered the blockage of flow by the air-throttling enhances fuel-air mixing and increases flow residence time by reducing flow speed. However, the auto-ignition is not fully established yet: it took a little more time. Plots at $t=4.5$ ms show the auto ignition of the mixture. While the pressure built up within 1 ms after fuel injection in

case of hydrogen injection, the delay is about 3 ms after air-throttling for ethylene fuel.

The pressure buildup by combustion leads to the shock-train (multiple-repeated oblique shocks) formation in the isolator section that moves forward to the exit of the facility nozzle. Then, air-throttling is deactivated, the exhaust process begins, and the situation before air-throttling is restored. Further details on each instance are discussed in the following section.

3.2 Flow characteristics at each instance

For further investigation of the flow structures, Mach number, density and pressure gradients are plotted. Sonic

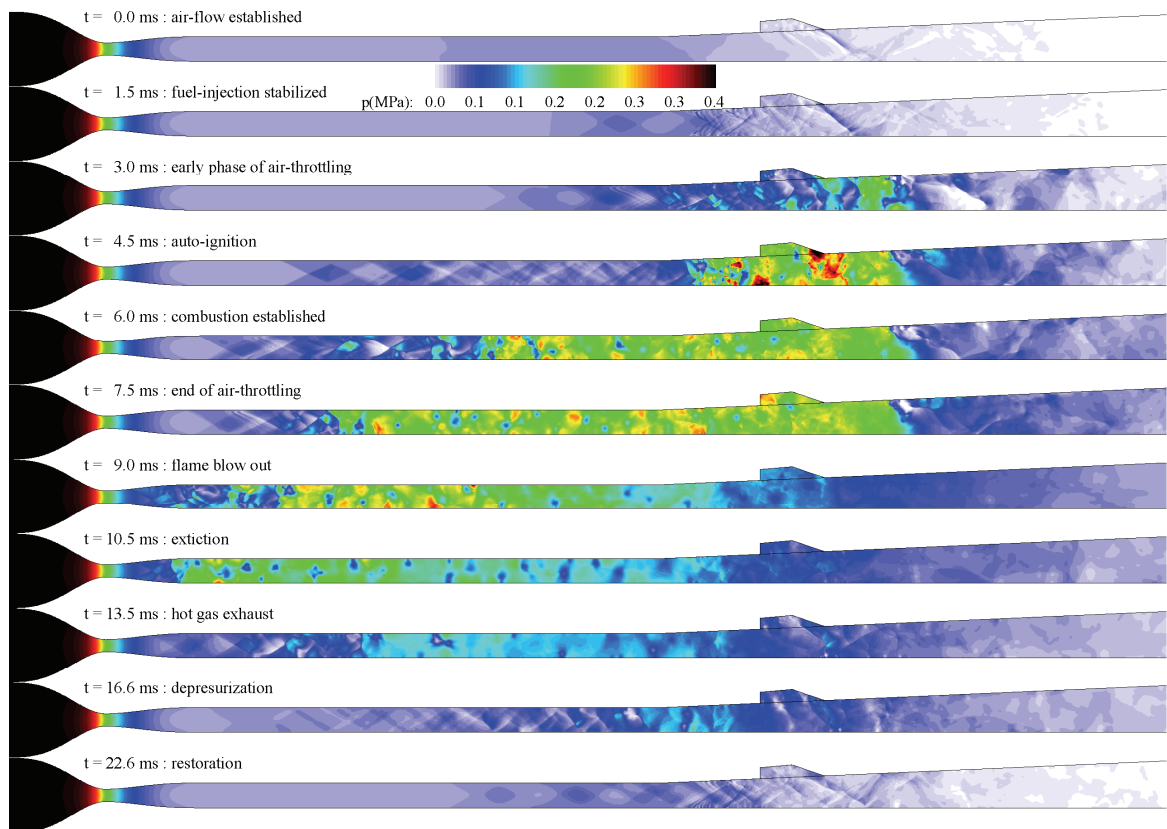


Fig. 3. Transients of pressure distributions.

lines are marked in black overlaid on the C_2H_4 mass fraction contours or magnified plots of pressure gradients. Fig. 4 contains the plots at $t=0.0$ ms. Magnified plots of density and pressure gradients are plotted in Fig. 5. Flow fields in isolator section shows a nearly steady state but the flow instabilities over the cavity resulted in complex wave interaction and reflection at the lower surface. Thus, flow does not reach the completely steady state but stabilized with oscillating supersonic cavity flows. The boundary layer is represented by the density gradients. The shock reflection results in separation bubble at lower surface, while the upper boundary layer is fluctuating downstream of the cavity. Supersonic flow is maintained throughout the combustor except the flow inside the cavity.

Figures 6 and 7 represent the flow field at 1.5 ms after fuel injection. Fluctuation of the fuel flow results in complex patterns of shock and expansion wave

interactions. The mass addition in the combustor reduced the effective flow area, resulting the increase of pressure and temperature and the decrease of the flow Mach number. It is shown that the flow around the fuel injector is maintained at subsonic speed which extended further upstream along the boundary layer. Thus, a crossing shock-train pattern is first established ahead of the combustor.

It is shown that the fuel flows along the surface, and quite a large amount of fuel resides within the cavity. The fuel does not mix sufficiently with air although the interface between fuel and air fluctuated. It does not lead to the combustion establishment over the combustor, although there is a very small amount of CO_2 mass fraction along the fuel layer. It is a different point from hydrogen, for which mixing and combustion is held instantly after the injection.

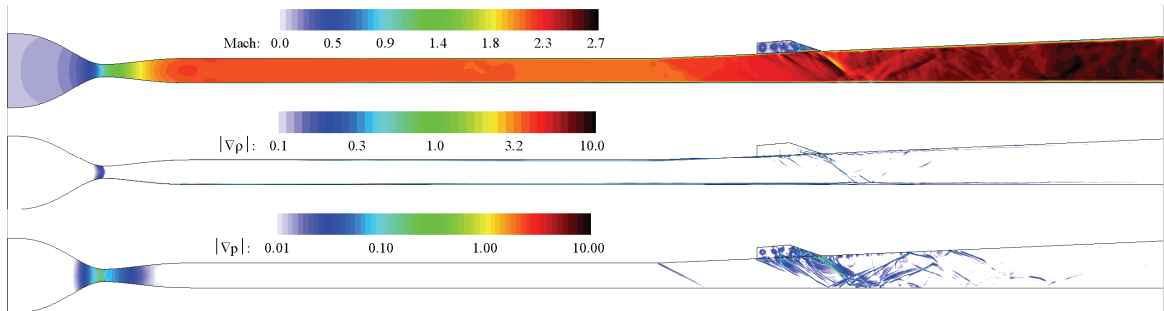


Fig. 4. Instantaneous contour plots at $t=0.0$ ms - air-flow established.

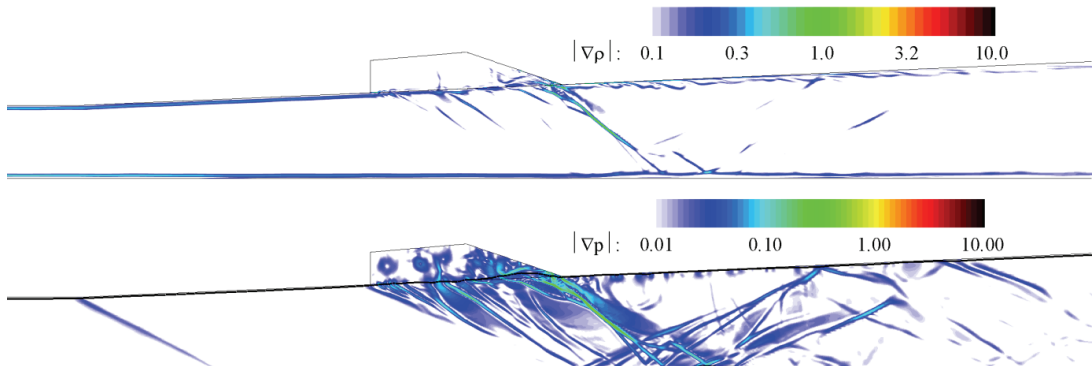


Fig. 5. Magnified plots of density and pressure gradients $t =0.0$ ms - air-flow established.

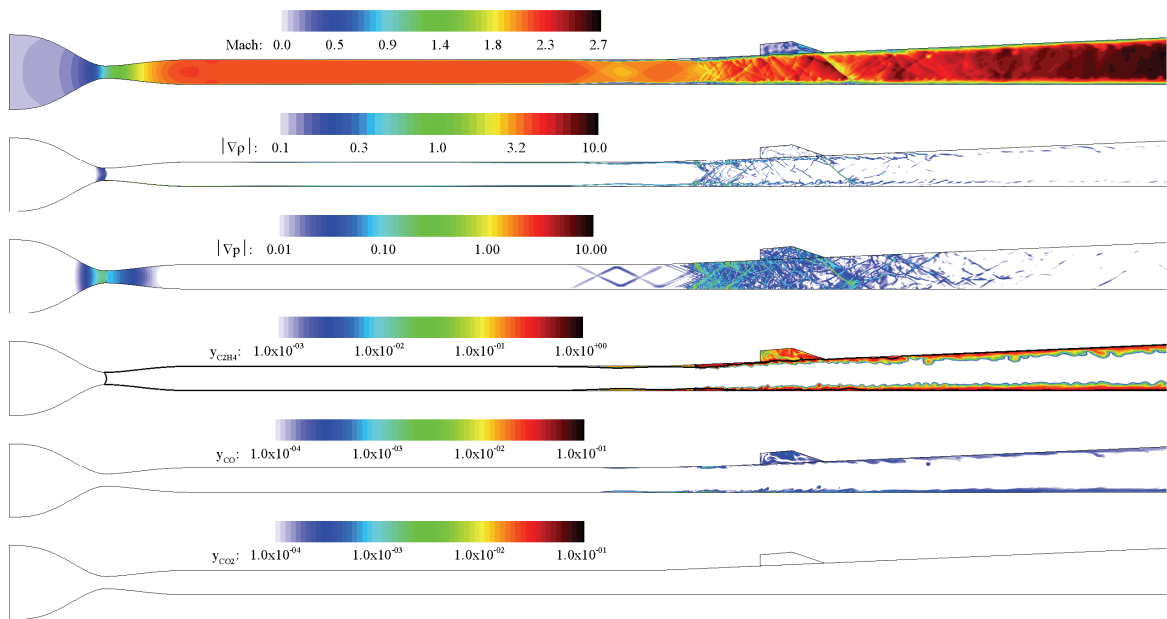


Fig. 6. Instantaneous contour plots at $t=1.5$ ms - fuel-injection stabilized.

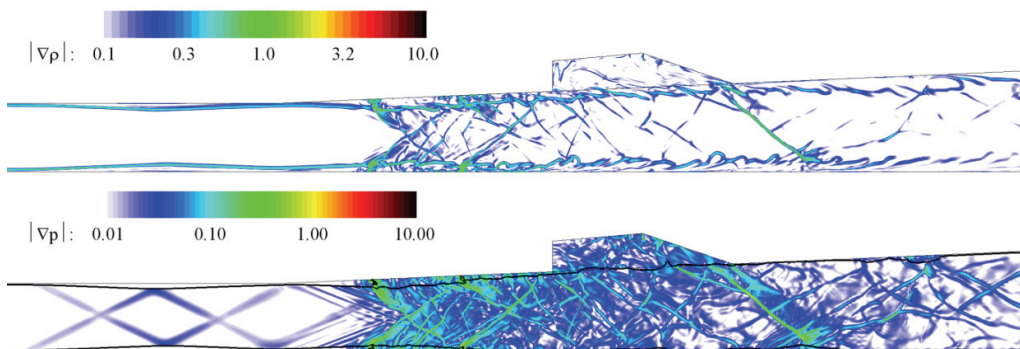


Fig. 7. Magnified plots of density and pressure gradients $t = 1.5$ ms - fuel-injection stabilized.

Figures 8 and 9 are plots at $t=3.0$ ms (1.5 ms after air-throttling). The mass addition by the air-throttle had a blockage effect on the air flow which resulted in a subsonic flow choked ahead of the air-throttle point, while supersonic flow is restored in downstream expansion region. Therefore, the flow residence time increases while the flow speed is reduced ahead of the air-throttling point. Resulting pressure increase facilitates the separation along the boundary layer, and the flow around the upper

injectors is submerged in the separated flow region. The boundary layer separation further reduces the effective flow passage area above the injectors. Pressure rises in this region pushes the shock-train to move forwards to the upstream location. Regardless of these air-throttling effects, the ignition is not sufficient, though the mass fractions of CO and CO_2 are increased higher but are less than 1% level.

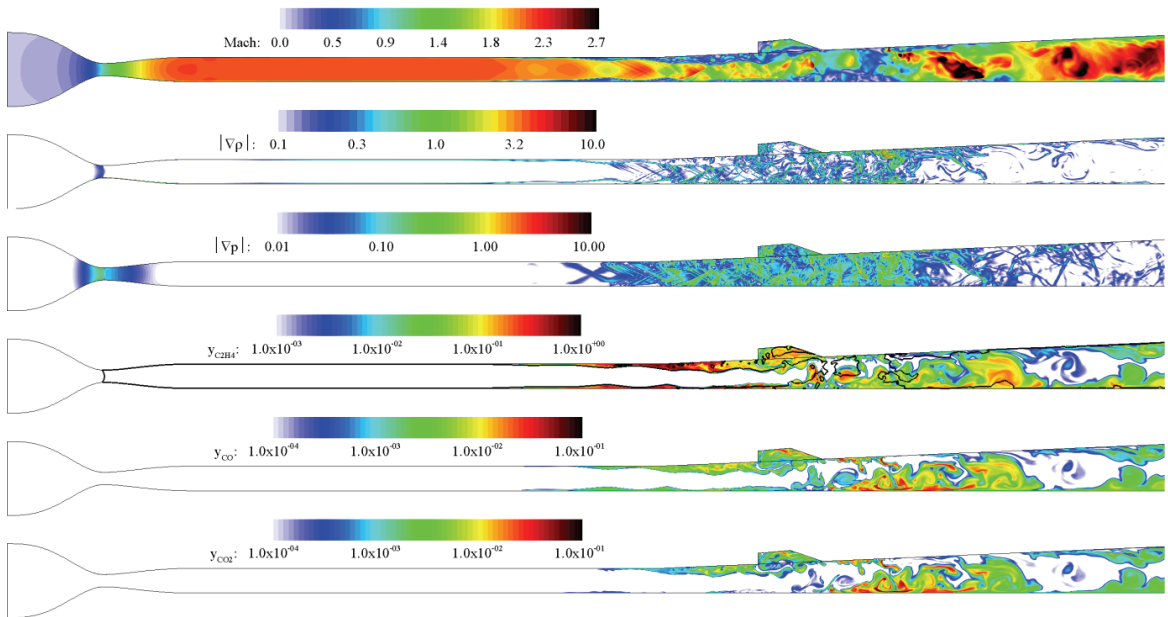


Fig. 8. Instantaneous contour plots at $t=3.0$ ms - early phase of air-throttling.

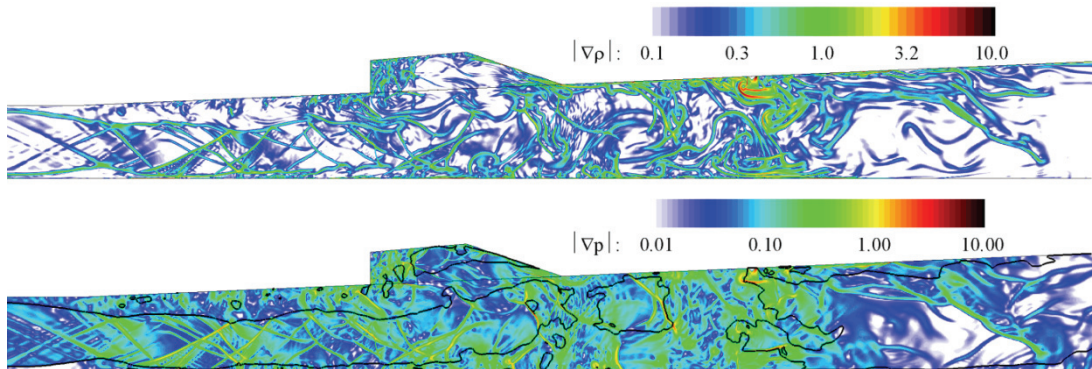


Fig. 9. Magnified plots of density and pressure gradients $t=3.0$ ms - early phase of air-throttling.

Figures 10 and 11 are plots of the instance at $t=4.5$ ms (3.0 ms after air-throttling). After experiencing the 3 ms of fuel-air mixing at reduced speed with heating, auto-ignition of the ethylene fuel takes place. The combustor region is kept subsonic starting from the fuel injectors to the air-throttling nozzle. The pressure is maintained at higher level over the entire subsonic region, but the combustion is anchored mainly over the cavity, where the

flow speed is reduced further. It is interesting that the cavity takes the role of subsonic flame holder with the presence of recirculation flow, mixing unburned and burned gases, facilitating the combustion.

The flow in isolator section is maintained at supersonic speed but the effective area is getting reduced by the back flow subsonic region. The shock-train advances upstream further with the extension of thickened boundary layer. A

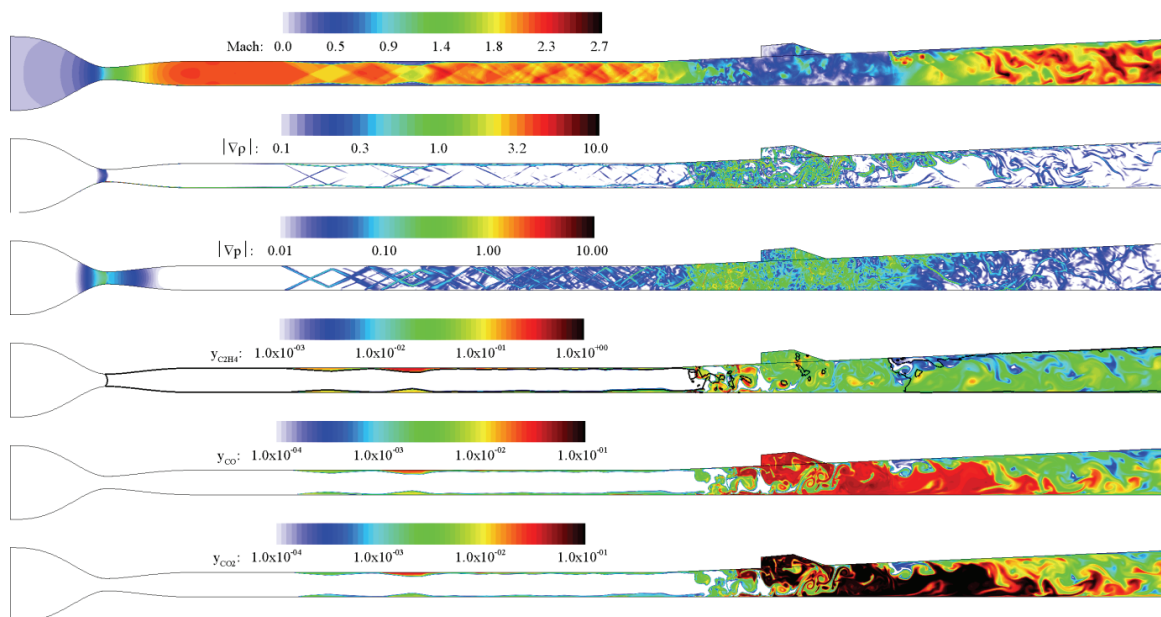


Fig. 10. Instantaneous contour plots at $t=4.5$ ms - auto-ignition.

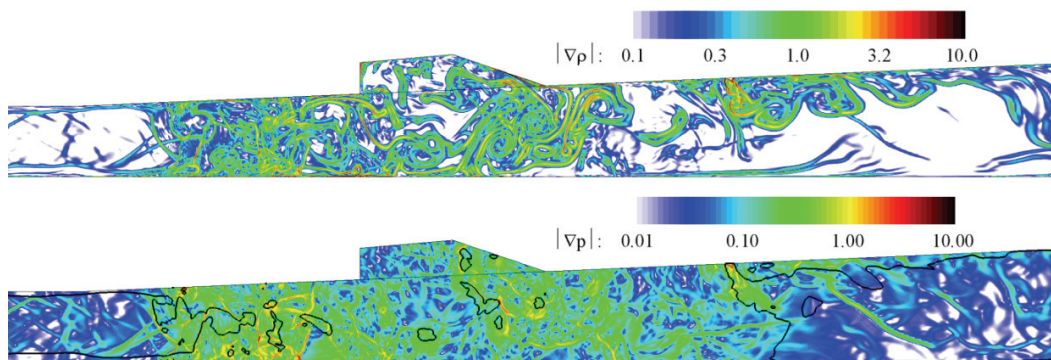


Fig. 11. Magnified plots of density and pressure gradients $t = 4.5$ ms - auto-ignition.

fraction of fuel and burned gas flows backwards through these boundary layers as noticed in the separation bubble at upper and lower surfaces. The interactions of the shock-train are more complex ahead of the injector, and the speed decreases to subsonic speed around the injectors.

Figures 12 and 13 are plots of the instance at $t=6.0$ ms (3.0 ms after air-throttling). Combustion is enhanced further, and the temperature rose, resulting higher level of CO mass fraction by dissociation. The amount of fuel

injection seems to be greater than that is necessary for the stabilization of the flow in the combustor. The pressure-rise in the combustor section extends the shock-train further upstream. The shock-train is about to reach the exit of the facility nozzle. The transition point of supersonic to subsonic flow exists in the middle of the isolator. The isolator flow exhibits subsonic vortical or tumbling motion after the transition point. The combustor flow is governed by these vortical motions, while the combustion

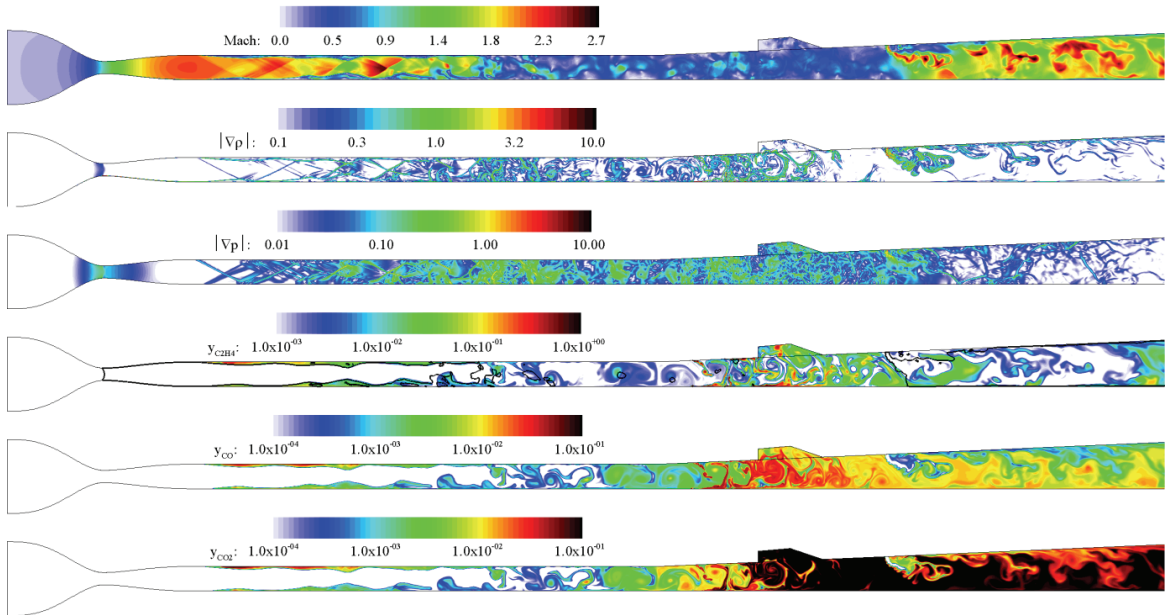


Fig. 12. Instantaneous contour plots at $t=6.0$ ms - combustion established.

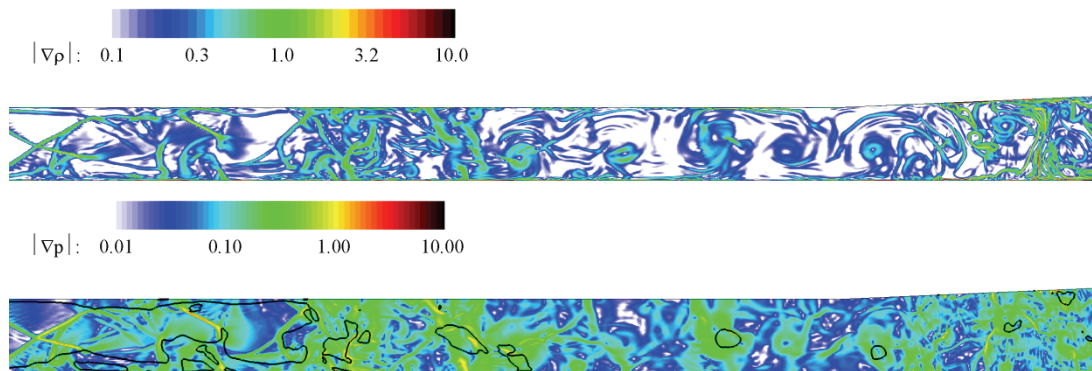


Fig. 13. Magnified plots of density and pressure gradients $t=6.0$ ms - combustion established.

is held mainly over the cavity.

Figures 14 and 15 are plots of the instance at $t=7.5$ ms just before the end of air-throttling. The shock-train extends further upstream due to the continuous pressurization in the isolator section. The subsonic transition point is located at the frontal part of the isolator, and the rest of the isolator section is occupied by subsonic flow. Since the vertical flow and tumbling motion are the

major features of the fluid dynamics in this subsonic region, the fuel injection is also affected greatly by these motions. Thus, the jet-in-crossflow feature of the injector flow disappears, but the fuel is injected almost vertically and mixed with air in vortical motion. Thus, the combustion is progressed above the injectors and an iota (less than 0.1 % in mass fraction) of the fuel and burned gas are present in the subsonic part of the isolator.

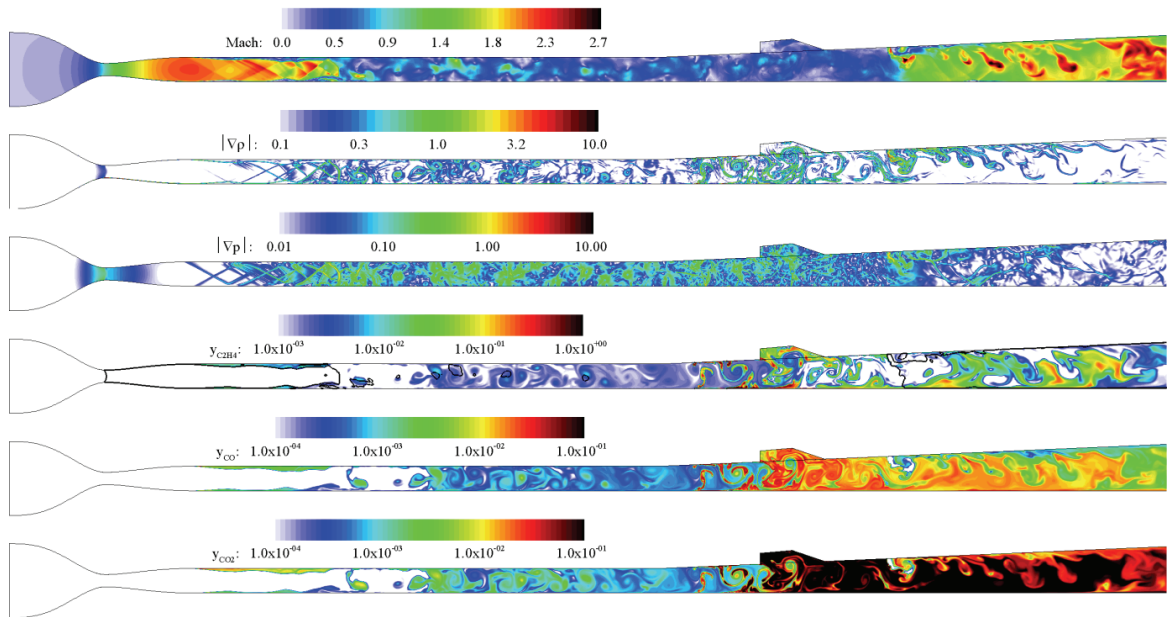


Fig. 14. Instantaneous contour plots at $t=7.5$ ms - end of air-throttling.

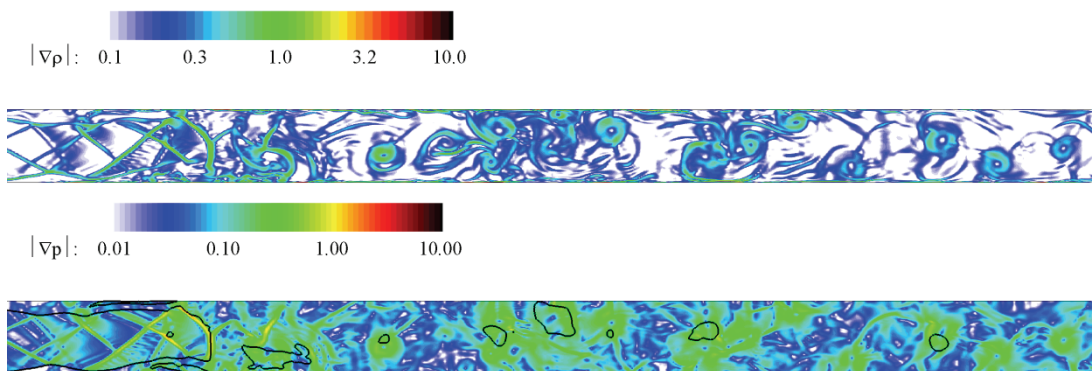


Fig. 15. Magnified plots of density and pressure gradients $t=7.5$ ms - end of air-throttling.

The instance at $t=9.0$ ms (1.5 ms after the end of air-throttling) is plotted on Fig. 16. Continuous pressurization in the isolator section further extends the shock-train forward. The shock-train is finally balanced at the exit of the facility nozzle due to the area contraction. This case could result in intake unstart if an ordinary supersonic inlet is used instead of the facility nozzle. The subsonic transition is followed by the large separation bubble at the

former part of the isolator, and the subsonic flow still occupies most of the isolator section. Since the blockage by the air-throttling is removed, the supersonic flow recovered at the expansion part of the combustor. The expansion in the combustor section resulted in the depressurization of the rear part of the isolator. The combustion region began to flow out of the combustor, even though the combustion is held inside the cavity.

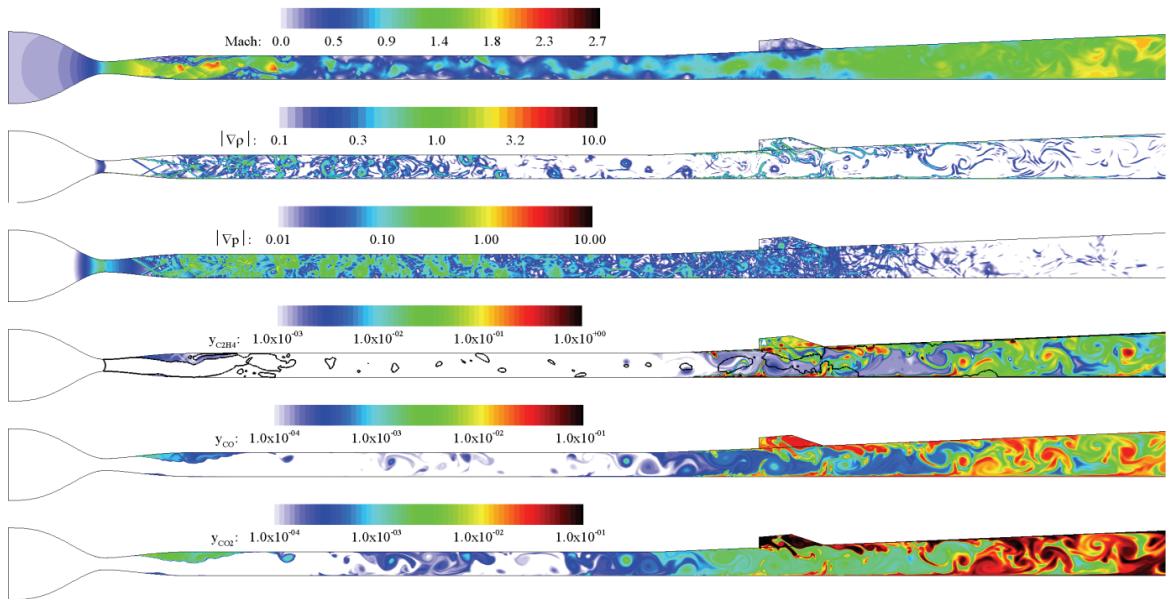


Fig. 16. Instantaneous contour plots at $t=9.0$ ms - flame blow out.

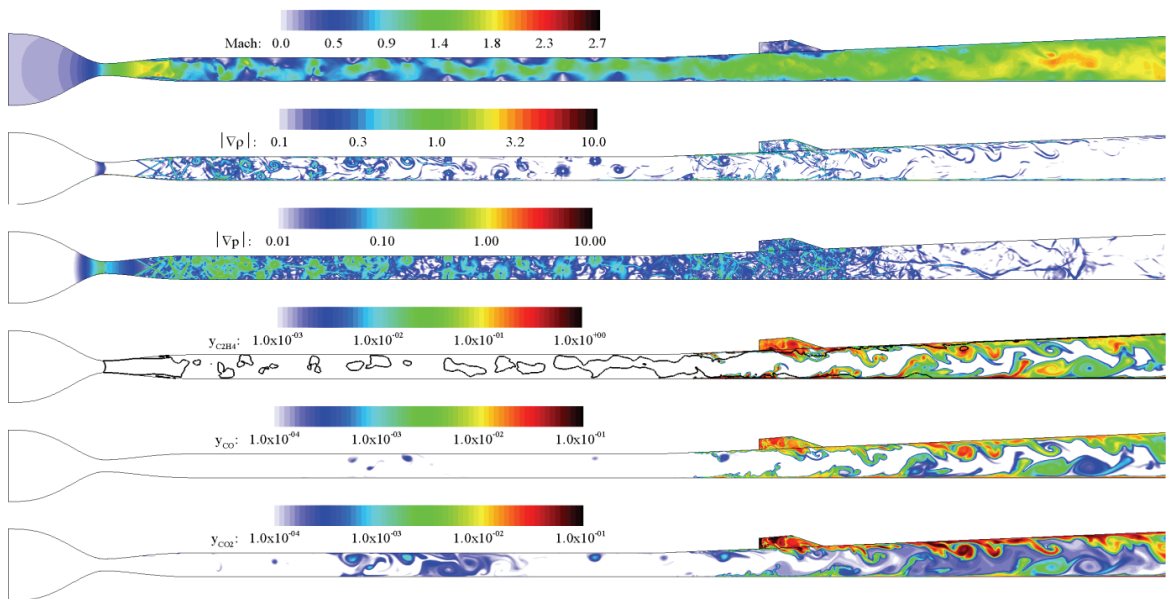


Fig. 17. Instantaneous contour plots at $t=10.5$ ms – extinction.

The instance at $t=10.5$ ms is plotted on Figure 17. Supersonic flow recovered over the entire combustor, but

the isolator is still occupied by subsonic flow with shock-train anchored at the frontal part of the isolator. The

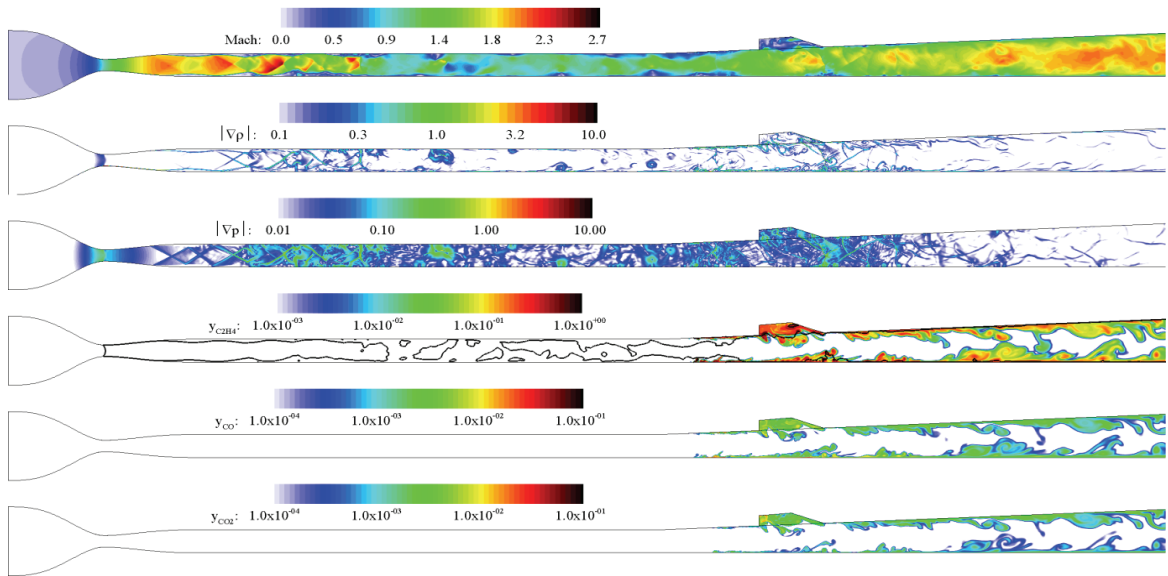


Fig. 18. Instantaneous contour plots at t=16.6 ms – depressurization.

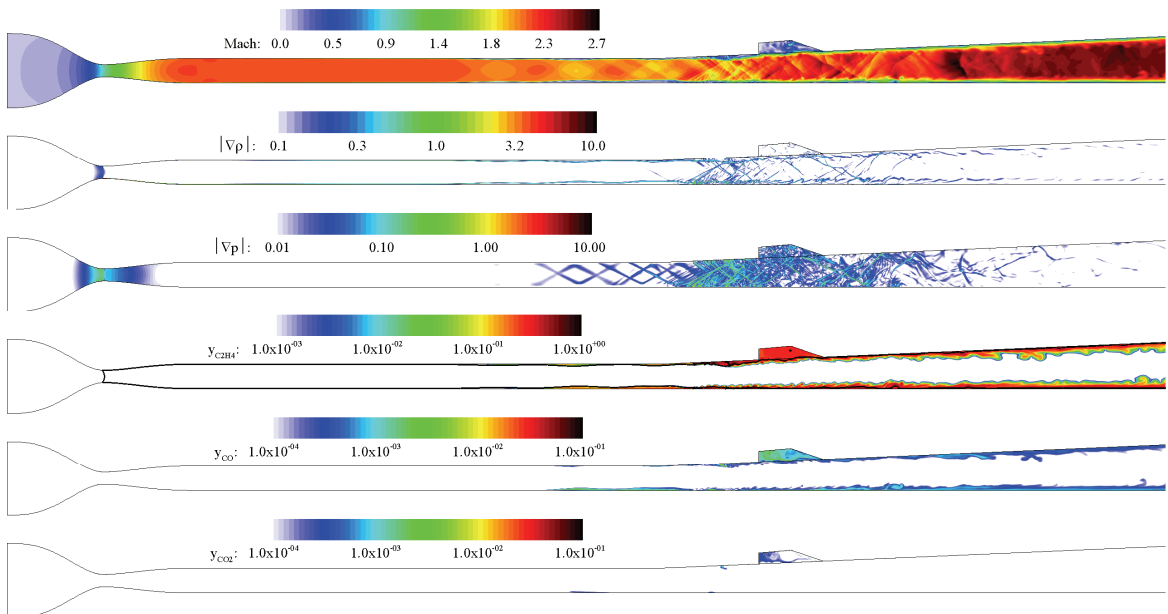


Fig. 19. Instantaneous contour plots at t=22.6 ms – restoration.

combustion is maintained within the cavity, but the mass fractions of fuel and reaction products are lowered significantly in the combustor. The flame is about to

quench, and the combustion is seemed not to be sustained any longer.

Figure 18 is the plotting of the instance at $t=16.6$ ms. The higher-pressure region in the former part of the isolator moves backwards due to the depressurization at the rear part. Supersonic flow is almost recovered in most of the combustor section. In the meanwhile, the cavity played the role of supersonic flame holder quite successfully, even though the level of the combustion product is reduced significantly. It looked like that only a small fraction of fuel is consumed by this supersonic combustion mode, resulting in very low combustion efficiency.

Figure 19 is the plotting of the instance at $t=22.6$ ms (after 15 ms after the end of the air-throttling). The flow structure is finally restored similarly to the situation before the air-throttling. The exhaust process takes much longer than forced pressurization with air-throttling. Though the cavity plays the role of the supersonic flame holder for a long period, it is considered insufficient to hold the supersonic combustion of ethylene for the conditions considered in this study. Two-dimensional configuration and combustion models of present study also could influence on this result.

4. Conclusion

A high-resolution numerical study is carried out to investigate the transient process of the fuel injection, combustion, and the shock-train formation by air-throttling in the isolator of an ethylene-fueled direct-connect scramjet combustor. The transient simulation begins with the supersonic air flow development followed by fuel injection. Air-throttling is then applied at the expansion part of the combustor to provide mass addition to block the flow to subsonic speed. The ignition occurs several milliseconds later when the fuel and air are mixed sufficiently. Due to the slower kinetics of ethylene reactions about 3 ms of delay is required before the combustion establishment of ethylene, which is quite a long time in comparison with the flow characteristic time of the scramjet combustor. The pressure buildup by the combustion leads to the shock-train formation in the

isolator section that advances to the exit of the facility nozzle. Then, the air-throttling is deactivated, the exhaust process begins and the situation before the air-throttling is restored. Present simulation shows the detailed processes in the dual mode scramjet combustor for better understanding of the operation regimes and characteristics. Air-throttling is confirmed to be an effective means of the ethylene ignition and combustion establishment. The cavity played a role of flame holder for broad range of flow speed from subsonic to supersonic. It is necessary to have further studies on the flame stabilization conditions including the amount of fuel injection and air throttling. Two-dimensional studies have shown to be effective to understand the various combustion flow features and operational characteristics in the dual mode scramjet combustor regardless of modeling limitations.

Acknowledgements

Publication of this research was supported by the Basic Research Program (Contract No. UD210020JD) of the Agency for Defense Development of the Republic of Korea.

References

1. Peebles, C., *Road to Mach 10: lessons learned from the X-43A flight research program*, Library of Flight Series, American Institute of Aeronautics and Astronautics, Reston, VA, U.S.A., 2008.
2. Hank, J.M, Murhy, J.S. and Mutzman, R.C., "The X-51A Scramjet Engine Flight Demonstration Program," 15th AIAA International Space Planes and Hypersonic Systems and Technologies Conference, Dayton, OH, U.S.A., AIAA 2008-2540, Apr. - May 2008.
3. Edwards, T., "Liquid Fuels and Propellants for Aerospace Propulsion: 1903–2003," *Journal of Propulsion and Power*, Vol. 19, No. 6, pp. 1089-1107, 2003.

4. Yang, V., Li, J. and Choi, J.-Y., "Ignition Transient in an Ethylene Fueled Scramjet Engine with Air Throttling Part I: Non- Reacting flow Development and Mixing," 48th AIAA Aerospace Sciences Meeting Including the New Horizons Forum and Aerospace Exposition, Orlando, FL, U.S.A., AIAA 2010-0409, Jan. 2010.
5. Donbar, J., Powell, O., Gruber, M., Jackson, T., Eklund, D. and Mathur, T., "Post-test Analysis of Flush-Wall Fuel Injection Experiments in a Scramjet Combustor," 37th AIAA/ASME/SAE/ASEE Joint Propulsion Conference and Exhibit, Salt Lake City, UT, U.S.A, AIAA 2001-3197, Jul. 2001.
6. Noh, J.-H., Choi, J.-Y., Byun, J.-R., Gil, H.-Y. and Lim, J.-S., "Numerical Study of the Auto-Ignition by Aero-throttling in an Ethylene Fueled Scramjet Engine," 46th AIAA/ASME/SAE/ASEE Joint Propulsion Conference & Exhibit, Nashville, TN, U.S.A., AIAA 2010-7036, Jul. 2010.
7. Noh, J.-H., Choi, J.-Y. and Yang, V., "Numerical Simulation of Ethylene Fueled Scramjet Combustor with Air Throttling, Part 1: Auto-Ignition," *Journal of Propulsion and Energy*, Vol. 1, No. 1, pp. 31-42, 2020.
8. Choi, J.-Y., Yang, V. and Ma., F., "Combustion Oscillations in a Scramjet Engine Combustor with Transverse Fuel Injection," *Proceedings of the Combustion Institute*, Vol. 30, No. 2, pp. 2851-2858, 2005.
9. Shin, J.-R., Moon, S.-H., Won, S.-H., and Choi, J.-Y., "Detached Eddy Simulation of Base Flow in Supersonic Mainstream," *Journal of The Korean Society for Aeronautical & Space Sciences*, Vol. 37, No. 10, pp. 955-966, 2009.
10. Won, S.-H., Jeung, I.-S, Parent, B., and Choi, J.-Y., "Numerical Investigation of Hydrogen Transverse Jet into Supersonic Crossflow using Detached Eddy Simulation," *AIAA Journal*, Vol. 48, No. 6, pp. 1047-1058, 2010.
11. Strelets, M., "Detached Eddy Simulation of Massively Separated Flows," AIAA Paper 2001-0879, 39th Aerospace Sciences Meeting and Exhibit, Reno, NV, Jan 8-11, 2001.
12. Vyasaprasath, K., Oh, S., Kim, K.S. and Choi, J.-Y., "Numerical Studies of Supersonic Planar Mixing and Turbulent Combustion using a Detached Eddy Simulation (DES) Model," *International Journal of Aeronautical & Space Sciences*, Vol. 16, No. 4, pp. 560-570, 2015.
13. Gruber, M., Donbar, J., Jackson, K., Mathur, T., Baurle, R., Eklund, D. and Smith, C., "Newly Developed Direct-Connect High-Enthalpy Supersonic Combustion Research Facility," *Journal of Propulsion and Power*, Vol. 17, No. 6, pp. 1296-1304, 2001.